11

Wavelets in Electrochemical Noise Analysis

Peter Planinšič[1] and Aljana Petek[2]
[1]*University of Maribor, Faculty of Electrical Engineering and Computer Science*
[2]*University of Maribor, Faculty of Chemistry and Chemical Engineering*
Slovenia

1. Introduction

Electrochemical noise (EN) is the term used to describe the spontaneous fluctuations of current or potential, which are generated during the corrosion processes. It has been investigated extensively since the 1968, and data has shown the use of EN measurements offers valuable sources of information about complex electrochemical reactions such as those in corrosion systems (Gabrielli et al., 1985; Bertocci & Huet, 1995) .
Many methods can be used to analyze the data, such as the variance, standard deviation and root mean square in the time domain. Alternatively, the signal has been transformed from the time domain to the frequency domain using fast Fourier transform or the maximum entropy method, giving the power spectrum density (PSD). The technique of wavelet analysis may be used instead, where a set of wavelets of varying amplitude, duration, and location be constructed such that reproduces the signal of interest.
Wavelets based methods are modern mathematical tools for multiscale time frequency analysis and characterization of in general nonstationary EN signals. This work presents the short overview to usability and possibilities of wavelet transformation in comparison with classic analysis.

2. Corrosion processes and electrochemical noise

Corrosion can be defined as the deterioration of materials due to its interaction with its environment and is appearing in various forms: as localized corrosion and as general (uniform) corrosion. Localized corrosion results in the accelerated loss of material at discrete sites in a passive materials surface, leading to the perforation or other failure. Since the majority of the surface is unaffected the difficulty with localized corrosion is its detection and prediction. Uniform corrosion results from the sites that are distributed randomly over the surface regarding both the space and time. Uniform corrosion damage is manifested in dissolving and the progressive thinning of a metal. To prevent corrosion or to predict the outcome of a corrosion situation the knowledge of mechanism of various form of corrosion is fundamental. Thermodynamic principles can be applied to determine which processes can occur and how strong the tendency is for changes to take place. Kinetic laws then describe the rates of the reactions.
Corrosion of metals in aqueous environments is electrochemical in nature. It occurs when two or more electrochemical reactions take place on a metal surface, producing dissolved

species of metal or solid corrosion products and thus lowering the energy of the system. The corrosion process has been written as two separate reactions occurring at two distinct sites on the same surface: the anode (metal dissolution site) and the cathode (site of the accompanying reduction reaction). At corrosion of iron in an acid solution containing dissolved oxygen, iron is oxidized to ferrous ion which passes into solution in the anode region

$$Fe \rightarrow Fe^{2+} + 2e^- \tag{1}$$

and H^+ ion is reduced to hydrogen or O_2 is reduced to water in the cathode region

$$2\,H^+ + 2e^- \rightarrow H_2 \tag{2}$$

$$O_2 + 4\,H^+ + 4e^- \rightarrow 2\,H_2O \tag{3}$$

The overall corrosion reaction is the sum of the anodic and cathodic partial reactions: sum of the reactions (1) and (2)

$$Fe + 2\,H^+ \rightarrow Fe^{2+} + H_2 \tag{4}$$

and sum of the reactions (1) and (3)

$$2\,Fe + O_2 + 4\,H^+ + 4e^- \rightarrow 2\,Fe^{2+} + 2\,H_2O \tag{5}$$

Electrochemical corrosion processes can be investigated by observation of charge flows between the electrolyte and the corroding metal. The measure of the rate at which reducible or oxidizable species can gain or lose electrons is the current density, j i.e. the charge flux trough a metal/electrolyte interface. The potential dependence of charge transfer rate is known as the Butler-Volmer equation:

$$j = j_0 \left\{ e^{(1-\alpha) f \eta} - e^{-\alpha f \eta} \right\} \tag{6}$$

where j_0 is exchange current density, α is transfer coefficient, η is overpotential, i.e. measure of how far the reaction is from equilibrium, and f is defined by:

$$f = \frac{nF}{RT} \tag{7}$$

where F is Faraday constant, R is the gas constant and T is the absolute temperature. If the Butler-Volmer equation is used to express the current densities in corrosion processes, the anodic reaction is the metal dissolution and the cathodic reaction is the accompanying reduction of H^+ or O_2. The equilibrium is achieved (the overpotential is zero) at the corrosion potential where no measurable current j flows: the anodic current density of metal dissolution must be equal to the cathodic current density and is equal to the corrosion current density, j_0. The overpotential is said to be positive if it is such as to produce a positive current, i.e. if it drives the anodic oxidation reaction and suppresses the reduction reaction.

In measurements procedure a potentiostat is often used and the electrochemical cell with tree electrodes: working electrode (WE) represents the interface of interest, the reference

electrode (RE) acts as standard for potential measurements and the counter electrode acts as electron sink or source for reactions that occur on the surface of WE. The potential of the WE is controlled with respect to the RE at a constant value, and the current density j under those conditions is determined. If the mean current is compensated or subtracted from the data and only random fluctuations are remained then electrochemical current noise is obtained. Electrochemical current noise thus can be measured as the random fluctuation in current of WE that is held at fixed potential or as the galvanic coupling current between two nominally identical working electrodes. Electrochemical potential noise is measured as the random fluctuation in potential of a WE with respect to a RE or as the fluctuation in potential difference between two nominally identical working electrodes.

In our investigations the current noise was monitored by a low-noise battery-operated potentiostat Jaissle IMP88 PC-R at a sampling rate of 10 points per second. The cell assembly was put in a Faraday cage. An example of measured time series for two processes (pitting as signal I_0 and general corrosion as signal I_2) is presented in Fig. 1. As is seen, the signal has a relatively smooth appearance for general corrosion and occasional sharp increases and decreases in the amplitude of current noise data occur for localized corrosion.

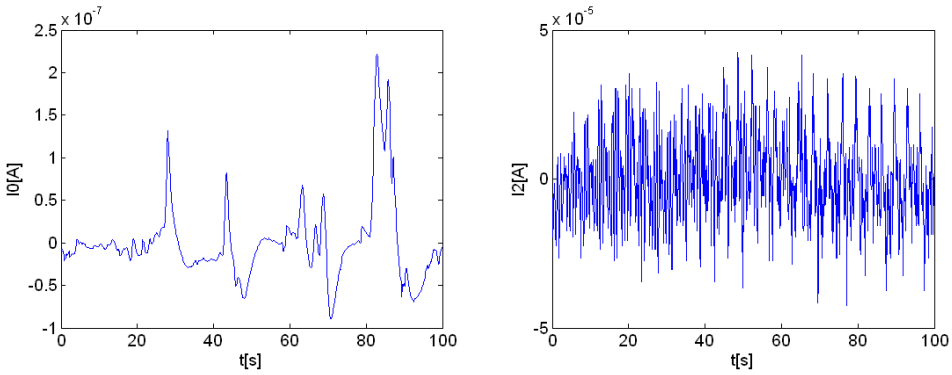

Fig. 1. Current noise signal corresponding to: a) X5CrNiMo17-13 stainless steel in borate buffer solution + 0.1 mol/dm^3 NaCl at the passive potential (I_0); b) Low Carbon Steel in 0.1mol/dm^3 H_2S0_4 at the corrosion potential (I_2) (Planinšič & Petek, 2008).

3. Stochastic processes and 1/*f* noise

EN-signals are generated from corrosion processes which are stochastic in their nature. A short theoretical overview of stochastic processes follows (Schroeder, 1991; Flandrin, 1992; Gao et al., 2007).

For understanding the stochastic processes it is essential to understand the concept of probability which is associated with random events. Often random events are presented by numbers, called a random variable. Let us denote a random variable by X, whose value depends on the outcome of random experiment ω. The probability $P(X < x)$ is denoted by $F_x(x)$ which is called the cumulative distribution function (CDF). When exist, it is usually more convenient to use its derivative $f_x(x)$, called the probability density function (PDF): $f_x(x) = dF_x(x)/dx$. Some commonly used distributions are normal or Gaussian

distributions, exponential and related distributions, binomial and related distributions and heavy tilled distributions. An important class of measures or parameters associated with CDF and PDF for a random variable is expected or mean value.
The mean or average of X can be obtained by relation:

$$E[X] = \overline{X} = \int_{-\infty}^{\infty} x dF_X(x) = \int_{-\infty}^{\infty} x f_x(x) \cdot dx \tag{8}$$

The p[th] order moment of X around zero is defined as:

$$E\left[X^p\right] = \int_{-\infty}^{\infty} x^p \cdot dF_X(x) = \int_{-\infty}^{\infty} x^p \cdot f_X(x) \cdot dx \tag{9}$$

The second moment represents the power of a random variable X.
The p[th] order central moment of X around mean value is defined as:

$$E\left[\left(x - \overline{X}\right)^p\right] = \int_{-\infty}^{\infty} \left(x - \overline{X}\right)^p \cdot f_X(x) \cdot dx \tag{10}$$

Variance of X is denoted as $Var(X)=\sigma_X^2$ and is the second order (p=2) central moment. The square rot of variance σ_X is called the standard deviation.
For a a given sample space S, a set of events E and a probability measure P, one can define a stochastic process as follows: For each sample point $\omega \in S$, we assign a time function $X(t,\omega)$. The stochastic process consists of the family of these functions. For each allowable parameter t, $X(t, \omega)$ is a random variable. For a fixed ω, $X(t, \omega)$ is a function of a time t; it is one realization of the stochastic process. There are many examples of stochastic processes. The well known examples are Markov processes and $1/f$ processes. We will focus our attention to $1/f$ processes. Stochastic process is also called a random process and for simplicity $X(t,\omega)$ is denoted as $X(t)$.
The activity of complex systems can usually be characterized by appearance of $1/f^{\beta}$ noise, a form of temporal fluctuations that has power-law power spectral density property over a wide range of frequencies. β is the power spectral exponent. A convenient framework for studying $1/f^{\beta}$ stochastic process is the self affine stochastic process $\mathbf{X} = \{X(t), t \geq 0\}$, which is defined by

$$X(\lambda \cdot t) \overset{d}{=} \lambda^H \cdot X(t), t \geq 0 \quad \lambda > 0, \quad 0 < H < 1 \tag{11}$$

where $\overset{d}{=}$ denotes equality in distribution, because of using the concept of statistical self similarity of time series. H is the Hurst parameter which is the measure of self-similarity. It can be derived, that a mean of such process is:

$$E[x(t)] = \frac{E[X(\lambda t)]}{\lambda^H} \tag{12}$$

the variance

$$Var\left[X(t)\right] = \frac{Var\left[X(\lambda t)\right]}{\lambda^{2H}} \tag{13}$$

and autocorrelation

$$R_{xx}(t,s) = \frac{R_{xx}(\lambda t, \lambda s)}{\lambda^{2H}} \tag{14}$$

By proving that $\lambda^{-H}X(\lambda t)$ and $X(t)$ have the same power spectral density, one can also prove that the power spectrum density of irregular, self similar processes has $1/f$ property:

$$S(\omega) \approx \frac{\sigma^2}{|\omega|^{\beta}} \qquad S(f) \approx \frac{\sigma^2}{|2\pi f|^{\beta}} = \frac{K \cdot \sigma^2}{f^{\beta}} \tag{15}$$

where ω is radial frequency, σ^2 is the variance, K constant value, and β the spectral exponent, which defines the slope of power spectral density over several decades.
An example of self-affine stochastic process is fractional Brownian motion process (fBm). It is nonstationary zero mean Gaussian process denoted as $B_H(t)$, characterized by scalar parameter H (Hurst parameter). The nonstrationary characteristic of fBm is evident from its covariance function structure:

$$E\left[B_H(t) \cdot B_H(s)\right] = \frac{\sigma^2}{2}\left(|t|^{2H} + |s|^{2H} + |t-s|^{2H}\right) \tag{16}$$

where E is the expectation operator. From this covariance function follows that the variance is of the type:

$$Var(B_H(t) = E\left[B_H(t)^2\right] = \sigma^2 |t|^{2H} \tag{17}$$

Although fBm process is nonstationary, it has stationary increments, which means that the probability properties of the difference process $B_H(t) - B_H(s)$ only depend on the lag t-s. It is this increment process which is self similar. The slope is in the range $1 \le \beta \le 3$. The slope β is 2 for the classic example Brownian motion.
The other example of $1/f^{\beta}$ processes is fractional Gaussian noise (fGn), with $-1 \le \beta \le 1$. fGn is stationary process. White Gaussian noise has the slope $\beta = 0$. It can be shown that Brownian motion ($\beta = 2$) is simply the integral of white noise.
It was reported, that β is related to the Hurst parameter H, which measures statistical self similar properties of signals:

$$\beta = 2 \cdot H + 1 \tag{18}$$

This is the reason for studying $1/f^{\beta}$ noise via self-affine stochastic processes. It was also shown, that for one dimensional signal, H is related to fractal dimension D by:

$$D = 2 - H \tag{19}$$

D is noninteger parameter in the range $1 < D < 2$ and H in the range $0 < H < 1$. The fractal dimension can also be used for characterizing the complexity of the stochastic signal.

Fractals are mathematical sets, which have a high degree of complex geometrical self similarity and can model many kinds of complex time series. The concept of statistical self-similarity and fractals was extended to time series to describe irregular characteristics of signals, from white noise to Brownian motion. The irregularity of a fractal curve or signal can be measured by capacity or fractal dimension D, a simplification of Hausdorf dimension, which is easier to calculate numerically. The roughness of such curve depends on D. The straight line have dimension 1. The more irregular the curve, the closer is its dimension to 2. There are many definitions and methods for calculation the fractal dimension. We will give a definition on which basis the popular box counting method.
Let S be a bounded set in $\Re^n$. The minimum number $N(s)$ of balls of radius s is needed to cover S; $N(s) \approx s^{-D}$. The fractal dimension is then defined as:

$$D = -\lim_{s \to 0} \inf \frac{\log N(s)}{\log(s)} \tag{20}$$

4. Classical statistical and Fourier analysis methods

In the past, the most common EN-analysis methods were statistical and Fourier methods. These methods assume the stationary or quasi stationary nature of processes and signals under consideration.
An early overview of different EN-data analysis methods was made in the work by R. A. Cottis (Cottis, 2001). Follows a little extended theoretical overview of classical methods (Orfanidis, 1996).

4.1 Background of statistical and Fourier methods

By analyzing random processes the statistical parameters as mean value and moments are defined by expectation operators, i.e. by statistical averaging of many realizations of stochastic process. In practice this is many times impossible and there is available only one block or array of N time signal samples. The statistical averaging is then replaced by the estimation obtained using sample or time average.
The p[th] moment of sample $x(n)$; n=0,..N-1 is defined as:

$$moment(p,x) = \frac{1}{N} \sum_{n=0}^{N-1} x^p(n) \tag{21}$$

The first moment is mean value $\bar{x}$. The square root of second moment gives the root mean square value x_{rsm}, which measures the amplitude of the signal. The square of x_{rsm} represents the signal power.
The p[th] central moment of sample is defined as:

$$central\_moment(p,x) = \frac{1}{N-1} \sum_{n=0}^{N-1} \left(x(n) - \bar{x} \right)^p \tag{22}$$

The second order central moment is the well known signal variance. The square root of variance is standard deviation, which is usually used for describing the amplitude of noise signals.

Classical spectral analysis bases on Fourier transform. The Fourier Transform of the deterministic continuous time signal $x(t)$ of duration T_1 is defined as :

$$X_{T_1}(j\omega) = \int_{T_1} x(t) \cdot e^{-j\omega \cdot t} dt \tag{23}$$

The Discrete Time Fourier Transform (DTFT) of the deterministic sampled signal with N samples is defined as:

$$X_N(\omega) = \sum_{n=0}^{N-1} x(n) \cdot e^{-j \cdot \omega \cdot n \cdot T} \tag{24}$$

where $x(n) = x(nT)$; n=0,1,…,N-1, is according to sampling theorem sampled analog signal $x(t)$, n is time index, and T the sampling period. It can be efficient computed by the Discrete Fourier Transform (DFT) and its fast version the Fast Fourier Transform (FFT).

$$X(k) = DFT\{x(n)\} = \sum_{n=0}^{N-1} x(n) \cdot e^{-j \cdot k \cdot n \cdot 2 \cdot \pi / N}; k = 0,1...,N-1 \tag{25}$$

where n is time index and k is the frequency index . The corresponding frequency resolution is given by:

$$\Delta\omega = \omega_s / N \tag{26}$$

where ω_s is radial sampling frequency. The main shortcoming of classical Fourier transform is the averaging the features across the whole time domain.
EN signals are of stochastic nature; therefore sampled EN signals are random sequences. To obtain smooth spectra an ensemble averaging should be introduced and the spectrum calculated over autocorrelation function. The autocorrelation function of a zero mean random signal is defined as:

$$R_{xx}(k) = E[x(n+k) \cdot x(n)] \tag{27}$$

where E is the averaging or expectation operator. For stationary signals, R_{xx} do not depend on time n, but only on the relative time lag k between sequences $x(n)$ and $x(n+k)$. The power spectrum of the random signal $x(n)$ is defined as the Discrete Time Fourier Transform (DTFT) of its autocorrelation function $R_{xx}(k)$:

$$S_{xx}(\omega) = \sum_{k=-\infty}^{\infty} R_{xx}(k) \cdot e^{-j \cdot \omega \cdot n \cdot T} \tag{28}$$

where ω is the frequency in radians per sec. This power spectrum shows how the power is spread over frequencies and is also called PSD (Power Spectral Density).
EN measurements cannot often be repeated to obtain smoothed spectra by ensemble averaging. One can compute an estimate of expected or true value by so-called sample autocorrelation using time average:

$$\hat{R}_{xx}(k) = \frac{1}{N} \sum_{n=0}^{N-1-k} x(n+k) \cdot x(n) \tag{29}$$

for k=0,1,…N-1. It is known that $\hat{R}_{xx}(k)$ is an even function of the lag k. It is also well known that the results are statistical reliable only for small value of lag (5 to 10 percentages).
The DTFT of $\hat{R}_{xx}(k)$ is $\hat{S}_{xx}(\omega)$ and is referred to as periodogram spectrum and can be viewed as an estimate of power spectrum:

$$\hat{S}_{xx}(\omega) = \sum_{k=-\infty}^{\infty} \hat{R}_{xx}(k) \cdot e^{-j \cdot \omega \cdot n \cdot T} \tag{30}$$

Using the above equations we can express the periodogram also as:

$$\hat{S}_{xx}(\omega) = \frac{1}{N} \cdot \left| X_N(\omega) \right|^2 \tag{31}$$

where $X_N(\omega)$ is DFTF of N signal samples. It can be efficient computed using FFT. For wide sense stationary random signals the mean of periodogram converges to the true power spectrum $S_{xx}(\omega)$ in the limit for large N:

$$S_{xx}(\omega) = \lim_{N \to \infty} E\left[\hat{S}_{xx}(\omega) \right] = \lim_{N \to \infty} E\left[\frac{1}{N} \cdot \left| X_N(\omega) \right|^2 \right] \tag{32}$$

There are some problems with such classical Fourier spectral analysis method. To achieve high statistical reliability, very long signal sequences should be used. But long signal sequences can no longer be stationary. However, the main shortcoming is the averaging the futures over the whole time domain.
This have lead researchers to find and develop of an advanced signal analysis methods. Recently wavelet based methods for signal analysis found to be useful for nonstacionary signals. Therefore in this overview chapter we will consider wavelet-based methods for EN-signals analysis.

4.2 Overview of works using classical methods

In individual systems, the correlations between noise measurements and corrosion processes have been reported by many authors but only some can be mentioned here. The EN data for a passive system (SS 316L/Ringer's solution) and several active systems (mild steel/NaCl, brass/NaCl, Al 6061/NaCl and Al 2024/NaCl) have been analyzed in the frequency domain using power spectral density (PSD) and spectral plots, obtained from the ratio of PSD plots of the potential and current fluctuations. Comparisons of spectral noise spectra with traditional impedance spectra have been made and good agreement has been observed for all systems after trend removal (Lee & Mansfeld, 1998; Mansfeld et al., 2001). Current fluctuation during general corrosion was analyzed upon a simple model, derived on the assumption that elementary fluctuation sources are related to the fluxes of electrons that are transferred from the metal to electron-acceptor ions in solution. The number of successful electron transfers obeyed a Gaussian distribution, from which the corrosion current density and transfer coefficients were determined (Petek et al., 1997; Petek & Doleček, 2001). The time-series noise patterns of the steel in bicarbonate solution (the simulated geological environment) were transformed into frequency domain by fast Fourier transformations, and then their power spectral densities at a frequency were determined to be compared with the corrosion rate (Haruna et al., 2003). Two new indices (S_E and S_G) were

derived to evaluate pitting corrosion by dimensional analysis of three parameters of PSD, the slope of high frequency linear region, the critical frequency and the low-frequency plateau level. As shown, the value of S_E can be related to the fluctuation velocity, which can represent the pitting corrosion rate and S_G should contain some information about slow corrosion processes (Shi et al., 2008). PSD had been employed to analyze EN data associated with corrosion behavior of A291D magnesium alloy in alkaline chloride solution. Three corrosion stages, the anodic dissolution process companying with the growth, absorption and desorption of hydrogen bubbles, the development of pitting corrosion, and the inhibition process by protective MgH_2 film could be distinguished. However, the results obtained only from PSD was insufficient for better understanding the corrosion mechanism of alloy during the immersion and the wavelet transform was carried out (Zhang et al., 2007).

4.3 Our applications of classical methods

EN signal (Fig. 1) is represented as a time series, where one can easily distinguish the fluctuations but not the intensity and frequencies of fluctuations. In the paper (Planinšič & Petek, 2003) we analyzed EN corrosion signals also with some classical methods, which use correlation functions and histograms. Figure 2 shows estimated autocorrelation functions of two corrosion signals I_0 and I_2, respectively.

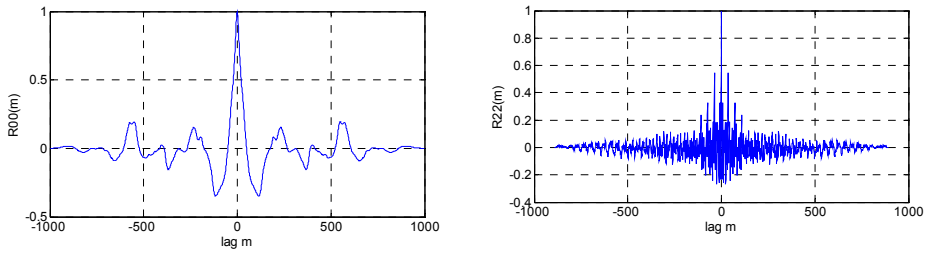

Fig. 2. Estimated autocorrelation functions of EN-signals: a) I_0; b) I_2

Noise data were transformed into frequency domain using FFT algorithm and presented as PSD in Figure 3. PSD of current noise data for pitting process exhibited two parts: a low-frequency plateau and high-frequency part, and the roll-off frequency, which is the frequency to separate the two parts of PSD. PSD plot of general corrosion can be characterized by "white noise" which is independent of frequency.

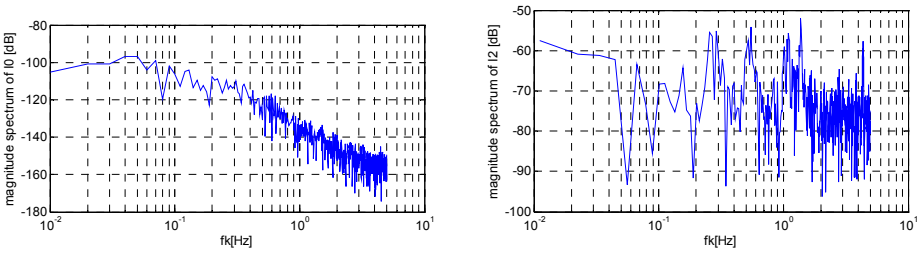

Fig. 3. Estimated power spectral density of signals I_0 (left) and I_2 (right)

Amplitude distribution was studied using normalized histograms. As demonstrated by Figure 4, a current noise amplitude distribution of general corrosion is Gaussian.

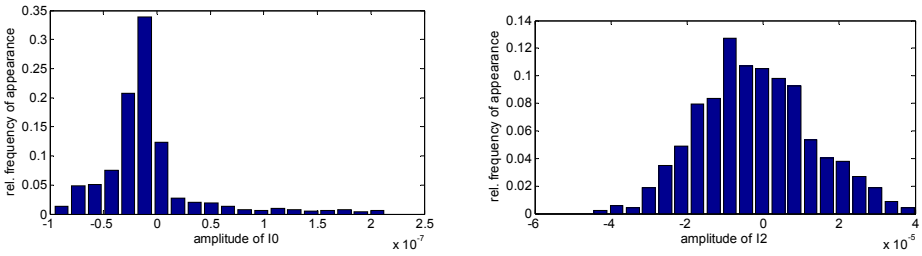

Fig. 4. Normalized histograms of signals I_0 (left) and I_2 (right)

5. Wavelet multiresolution analysis methods

The assumption of stationary behavior of corrosion processes and random signals is not always correct. Corrosion signals are a non stationary in general.

When we are interested on how signal frequency components vary with time, we should use joint time-frequency analysis. For this purpose we can use Window Fourier Transform (WTF), also called Short Time Fourier Transform (STFT) or spectrogram. It is known that the STFT can be considered as the filter bank, consists of Finite Impulse Response Filters (FIR) with equal bandwidth or equal frequency resolution. Therefore it is difficult to meet sharp localization in time and frequency simultaneously. For this reason, this technique is not always appropriate for analyzing natural signals or phenomena, where in the signal exist long duration low frequency components and short high frequency components at the same time. This problem can be elegantly solved using modern multiresolution time frequency analysis methods based on wavelets. It was shown that the Discrete Wavelet Transform can be viewed and realized as multirate filter bank with octave, also called constant Q frequency resolution.

A short theoretical overview of wavelet methods follows (Daubechies, 1992; Burrus, 1992; Fladrin,1992, 1993; Radolphe, 1994; Wornell, 1996; Mallat, 1998; Dai et al., 1994; Palawajjhalla et al., 1994).

5.1 Background of wavelet methods

Wavelets are waves which construct basis of signal decomposition in wavelet transforms, similar as trigonometric functions with different frequencies in Fourier Transform. Wavelets are scaled and shifted versions of the so called mother or primary wavelet function $\psi(t)$. Thus the family of functions is then defined as:

$$\left\{\psi_{a,b}(t)\right\}; \quad \psi_{a,b}(t) = |a|^{(-1/2)} \cdot \psi\left(\frac{t-b}{a}\right) \tag{33}$$

where parameters a and b $(a,b \in \Re; a \neq 0)$ are called dilation (scaling) and translation (shifting) parameters, respectively. To be a good analyzing function, the mother wavelets must fulfill some conditions. The first is the so called ''admissibility'' condition:

$$\int_{-\infty}^{\infty} \frac{|\hat{\psi}(\omega)|^2}{|\omega|} \cdot d\omega < \infty \tag{34}$$

where $\hat{\psi}(\omega)$ is the Fourier transform of $\psi(t)$. Because the mother wavelet is absolutely inferable functions, we can show that:

$$\hat{\psi}(0) = 0 \Leftrightarrow \int_{-\infty}^{\infty} \psi(t) \cdot dt = 0 \tag{35}$$

Admissibility implies that a wavelet must be an oscillatory decaying function with zero mean. There are also additional other desirable properties for a function to be a useful wavelet, as smoothness, good time and frequency localization, number of vanishing moments. These properties suggest that wavelets are bandpass filters. $\psi(t)$ is the impulse response of filter $\hat{\psi}(\omega)$.

In the contrast with Fourier analysis where basis functions are trigonometric functions, by wavelet-based analysis different kind of mother wavelet function can be used, appropriate for particular application. There are many types of wavelet transforms according to input signals, time and scaling parameters, used wavelet functions, namely continuous, discrete, bi-orthogonal and semi-orthogonal and orthonormal bases version.

However wavelet transform can be broadly classified into Continuous Wavelet Transform (CWT) and Discrete Wavelet Transform (DWT). CWT of a function $f(t) \in L^2(\Re)$ involves the computation of scalar product. Wavelet coefficients are computed as:

$$C_{a,b} = C(a,b) = \int_{-\infty}^{\infty} f(t) \cdot \psi_{a,b}(t) \cdot dt \tag{36}$$

Discrete wavelet transform involves discretization of parameters, *a* and *b*, respectively:

$$a = a_0^{\ m} \qquad b = n \cdot b_0 \cdot a \tag{37}$$

$$\psi_{m.n}(t) = a_0^{\ -m/2} \psi(a_0^{\ -m} \cdot t - n \cdot b_0) \tag{38}$$

$$C_{m,n} = \left\langle f(t), \psi_{m,n}(t) \right\rangle = \int_{-\infty}^{\infty} f(t) \cdot \psi_{m,n}(t) \cdot dt \tag{39}$$

where $C_{m,n}$ are called discrete wavelet coefficients. Discrete wavelets $\psi_{m.n}(t)$ that satisfy the condition:

$$A \cdot \|f(t)\|^2 \le \sum_{m,n} \left| \left\langle f(t), \psi_{m,n}(t) \right\rangle \right| \le B \cdot \|f(t)\|^2 \tag{40}$$

are called frames (Daubechies,1992) and form Riesz basis. Discrete wavelets can be further classified into orthogonal, semi-orthogonal or non-orthogonal.

To obtain orthonormal basis, one can chose samples on dyadic grid (base 2):

$$a = 2^m \qquad b = n \cdot 2^m \qquad m \in \mathrm{Z}, n \in \mathrm{Z} \tag{41}$$

Orthonormal bases and orthonormal wavelet transform, play an important role in theory and practice of multiresolution analysis. The DWT can be further classified into Wavelet Series Transform (WST), when analyzed signal is continuous ($f(t)$), and into Discrete Time Wavelet Transform (DTWT), if the signal is time discrete ($f(n)$). One possibility of constructing wavelets is using a scaling function $\phi(t)$ and multiresolution analysis (Mallat, 1998). Namely, multiresolution algorithm is a natural way of constructing orthogonal wavelets. Multiresolution analysis is decomposition of square integrable functions $f(t) \in L^2(\Re)$ into closes subspaces V_j , where coarser subspace V_j is contained in finer subspace V_{j+1}: $V_j \subset V_{j+1}$. The subspaces also satisfy separation condition ($\underset{m \in Z}{\cap} V_m = \{0\}$) and condition for completeness ($\underset{m \in Z}{\cup} V_m \in L^2(\Re)$. Additionally, the functions $f(t)$ satisfy the scaling property ($f(t) \in V_m \Leftrightarrow f(2t) \in V_{m-1}$). And, there exist a scaling function in the coarsest space $\phi(t) \in V_0$, so that the family of functions $\{\phi_{m,n}\}$, $\phi_{m,n} = 2^{-m/2}\phi(2^{-m}t - n)$, form the so called Riesz basis of subspace V_m. Since $\phi(t) \in V_0 \subset V_1$ and the $\phi(2t)$ is a basis for the subspace V_1 , we can write scaling function as linear combination with the so called two scale difference equation:

$$\phi(t) = \sum_k h(k) \cdot \phi(2t - k) \tag{42}$$

where $h(k)$ is a finite sequence. It can be shown, that the frequency response of scaling function is a lowpass filter and $h(k)$ form the lowpass FIR-filter coefficients. Define W_{m-1} as the orthogonal complement of subspace V_{m-1} in V_m , than the direct sum of infinite subspaces V_j is the whole space $L^2(\Re)$. The subspace W_{m-1} contains the detail information needed to go from approximation of function at coarser to finer resolution level j. The multiresoluton analysis allows to approximate the given function $f(t)$ by $f_j(t)$ at each coarser subspace or resolution level. If $\psi(t)$ is a Riesz basis of space $W_0 \subset V_1$, we can also write:

$$\psi(t) = \sum_k g(k) \cdot \psi(2t - k) \tag{43}$$

where the finite sequence $g(k)$ form the highpass (bandpass) filter coefficients, as the frequency response of wavelet is like that of band-pass filter.
The multiresolution analysis form the theoretical basis for fast Discrete Wavelet Transform (fast DWT), using discrete signals $f(n)$, $n \in Z$, that is sampled version of $f(t)$. It was introduced by Mallat by the so called pyramidal multiresolution algorithm, where the signal $f(n)$ is decomposed into J decomposition levels. The idea of multiresolution analysis is to write a function as a limit of successive approximations, each of which is a smoothed version.
The sequences at scale j can be computed from sequences at scale j-1 by the following multirate filter or convolution, followed by subsampling by 2:

$$\begin{aligned} a_{2^j}(n) &= \left\langle f(t), \varphi_{m,n}(t) \right\rangle = \sum_k g(k - 2^j \cdot n) \cdot a_{2^{j-1}} \\ c_{2^j}(n) &= \left\langle f(t), \psi_{m,n}(t) \right\rangle = \sum_k h(k - 2^j \cdot n) \cdot a_{2^{j-1}} \end{aligned} \tag{44}$$

where $c_{2^j}(k) = c(j,k)$ are wavelet or detailed coefficients and $a_{2^j}(k) = a(j,k)$ are scaling or approximation coefficients. Data sequence $a_{2^1}(k) = a(1,k)$ at scale j=1 represents approximated or smoothed version of the original signal. The sequence $c_{2^1}(k) = c(1,k)$ at level j = 1 represents difference or detail information. The above equations together describe j^{th} level analysis filter bank. This calculation is repeated (iterated) up to scale J forming the multiresolution pyramidal algorithm; one stage is shown in Figure 5. As was mentioned, the lowpass filter is associated by scaling function and highpass filter by wavelet function. The filters for calculating the synthesis are the same by using orthogonal wavelet transform. Analysis and synthesis filters can have different length, as by using biorthogonal filter banks. However, this algorithm can be used for orthogonal and nonorthogonal wavelets.

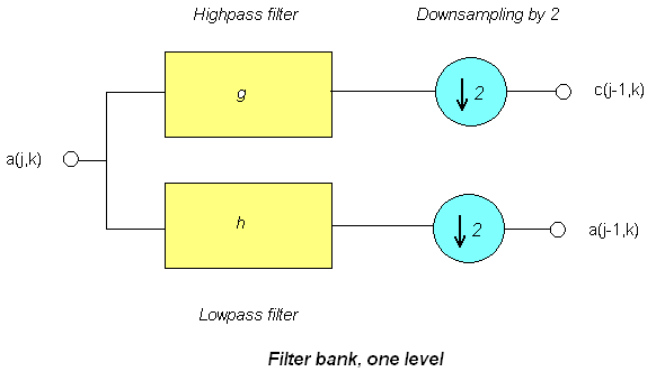

Fig. 5. One stage of analysis filter bank

For EN-signal originating from corrosion process, wavelet transform decompose it into approximation and detail signal components at different scales and locations. The wavelet transform is therefore convenient tool to analyze the self-similarity of 1/f time series.
The orthonormal wavelet transform based methods were used for estimating slope β, parameter H, and fractal dimension D (Akay,1998; Sekine, 2002; Planinšič & Petek, 2008). For orthonormal discrete wavelet decomposition the 1/f property can be replaced by the relation:

$$\sigma_j^2 = \frac{\sigma^2}{\left(2^j\right)^{\beta}} \tag{45}$$

where σ_j^2 is the variance of detail signal d_{2^j}. Then the slope β can be calculated from the plot $\log_2 \sigma_j^2$ versus level j, what can be obtained after short calculation:

$$\log_2 \sigma_j^2 = -\beta \cdot j + \log_2 \sigma^2 \tag{46}$$

5.2 Overview of works using wavelets

Wavelets have found many applications in different natural scientific disciplines, among them also in chemical engineering (Radolphe et al., 1994; Banjanin et al., 2001). The use of

wavelets to study electrochemical noise transients was reported by Aballe (Aballe et al., 1999; 2001). The wavelet analysis of electrochemical noise signals, where the signal was decomposed into wavelet-subbands was used for the characterization of pitting corrosion intensity (Smulko et al., 2002). Wharton et al. demonstrated how the wavelet variance exponent can be used to evaluate corrosion behavior for variety of stainless steels in chloride medium, i.e. be able to discriminate between various corrosion processes covering a wide range of EN signals (Wharton et al., 2003). Wavelet analysis based on the fractional energy contribution of smooth crystals and the lowest frequency detail crystal can provide information on the type and onset of corrosion (general corrosion, metastable pitting, stable pitting) in performed potentiostatic critical pitting temperature test for a superduplex stainless steel (Kim, 2007). In study of the copper anode passivation by electrochemical noise analysis using wavelet transforms it has been found that during active dissolution the electrode surface is dominated by long time scale process and the change of the position of the maximum relative energy from D7 to D8 could be an indication of future passivation (Lafront et al., 2010). It was shown, that electrochemical potential noise analysis of Cu-BTA system using wavelet transformation can be used to achieve the inhibition efficiency (Attarchi et al., 2009).

Some other authors also reported about the fractal nature of corrosion processes and corresponding electrochemical noise signals. The electrochemical potential and current noise originating from the corrosion of carbon steel in distilled water was analyzed using multifractal analysis. The multifractal spectra are found to be qualitatively different for different temporal stages of the corrosion process (Muniandy et al., 2011).

5.3 Our applications of wavelets methods

Our applications of wavelets transformation or combination with classical methods for the electrochemical current noise analysis were reported for different corrosion processes in several publications (Planinšič & Petek, 2003; 2004; 2007; 2008). For little more detailed insight the short overview of this research is as follows.

Daubechies wavelets ''db2'' were used to transform the EN signal from Fig. 1. The discrete wavelet transform (DWT) decomposition of signal into on joint time (position) and frequency (scale level) depended amplitudes are presented with color lightness in time-frequency plane in Fig. 6.

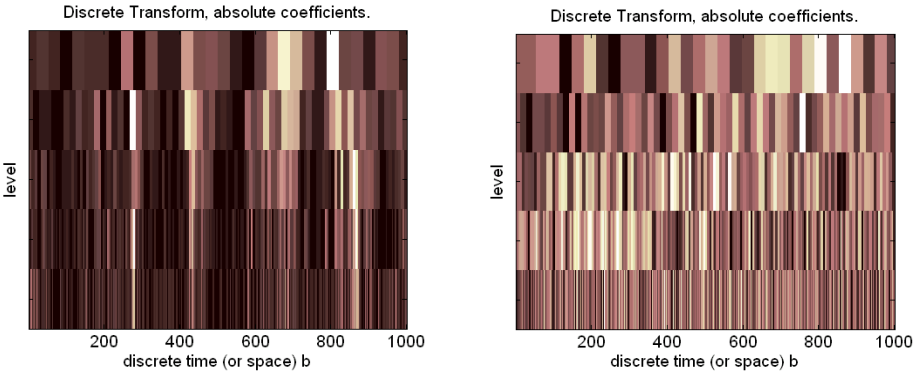

Fig. 6. Discrete wavelet transforms (DWT) of signals: a) I_0, b) I_2 (Planinšič & Petek, 2008)

Next, the DWT multiresolution decomposition of processes on 5 levels are shown in Fig. 7. The crystals from D_1 to D_5 are the details of the signal, and A_5 is the approximation of the signal. The frequency range which takes into account each series of detail coefficients, can be computed from relation $f_s / 2 / 2^j$ where f_s is the sampling frequency and j stands for the corresponding scale.

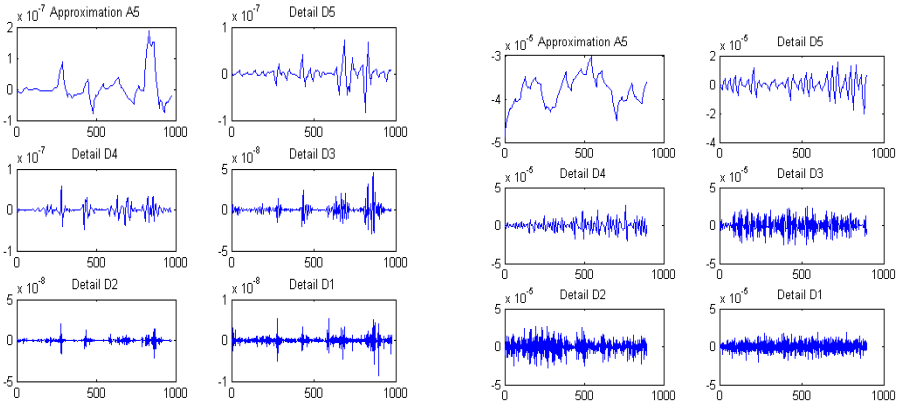

Fig. 7. Multiresolution decomposition of discrete signals: a) I_0, b) I_2 on approximation signal A_j and detail signals D_j on five levels (Planinšič & Petek, 2008).

Events with small time constants are taken into account by the fine scale coefficients, details D_1, D_2. The information dealing with larger time constant events is included in details D_4 and D_5. Therefore, these kinds of plot allow the signal to be viewed over the full time range and considering different scales, which contains information about corrosion events occurring at a determined time – scale.

Variances of details were calculated to detect the intensity of particular signal components on level j. Fig. 8 shows variances as a function of the decomposition level and also the logarithmic plot of details variances versus level j for the slope $ß$ determination.

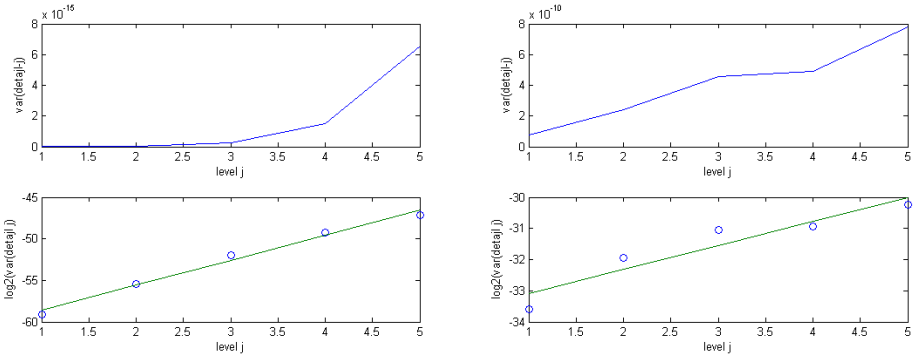

Fig. 8. Variances of details plotted as a function of the decomposition level j for two processes: a) I_0 (slope $ß$ = 3.0092) and b) I_2 (slope $ß$ = 0.7700) (Planinšič & Petek, 2008).

For the time series I_2 and I_0 were $ß$ = 0.7700 and $ß$ = 3.0092, respectively. As the value of $ß$ increases, the contributions of high-frequency components in time series are reduced. It is suggested that the events in the relatively higher frequency region may be associated with uniform corrosion. On the other hand, the events in the relatively lower frequency regions are responsible for pitting corrosion.
After short computation the value for Hurst parameter H, and fractal dimension D can be obtained:

$$D_i = 2,5 - 0,5 \cdot \beta_i \qquad H_i = 0,5 \cdot (\beta_i - 1); \quad i = 1,2. \tag{47}$$

The obtained slope $ß$ is the estimated power spectral exponent $ß$. It can be associated with the strength of persistence within a time series. The persistence defines the correlation between adjacent values within time series. If $0 \le \beta \le 1$, than persistence is weak. For the time series with β between 2 and 3, the persistence is strong. Fractional Gaussian noise with β between -1 and 1, and fractional Brownian motion, with β between 1 and 3, are considered as proper representatives of such processes. The first process is stationary and the second is non-stationary.
The obtained results indicating the presence of fractional Brownian motion in pitting corrosion with adjacent values in the time series being strongly correlated and fractional Gaussian noise in general corrosion, with adjacent values in the time series being weak correlated. The Hurst parameter in case of pitting is greater than ½, indicating also the persistence, i.e. a dependence of new values on old values. A summary of the wavelet – based fractal analysis is given in Table 1.

	β_i	H_i	D_i	process	persistence
I_0 – pitting corrosion	3.0092	1.0046	0.9954	non-stationary	strong
I_2 – general corrosion	0.7700	-0.1150	2.1150	stationary	weak

Table 1. The slope β, the Hurst parameter H, and the fractal dimension D, for two corrosion signals (Planinšič & Petek, 2008).

We proposed also a new way for determination of persistence nature of the electrochemical noise on the basis of correlation coefficients between original signal and details $R(I_i,D_j)$, Table 2. The pitting corrosion is positively correlated with long memory effect. Increasing correlation of signal I_2 to the D_2 detail and then decreasing to D_5, indicates weak persistence and short memory effect of general corrosion processes.

	$R(I_0,D_j)$	$R(I_2,D_j)$
D_1	0.0188	0.4196
D_2	0.0482	0.5303
D_3	0.1128	0.5097
D_4	0.2048	0.3648
D_5	0.3103	0.3138

Table 2. Correlation coefficients between original signal and details, $R(I_i,D_j)$, for two decomposed corrosion signals (Planinšič & Petek, 2008).

Correlation coefficients between successive details $R(D_j,D_{j+1})$ for two decomposed corrosion signals (Table 3) are all zero on the basis of analysis procedure.

	I_0	I_2
$R(D_1,D_2)$	0.0006	0.0006
$R(D_2,D_3)$	0.0000	0.0004
$R(D_2,D_3)$	0.0001	0.0004
$R(D_4,D_5)$	-0.0012	-0.0120

Table 3. Correlation coefficients between successive details, $R(D_j,D_{j+1})$, for two decomposed corrosion signals (Planinšič & Petek, 2008).

Additionally, DWT with 3-decomposition levels was made using different kinds of wavelet functions, from Daubechie's fractal-like wavelet "db2" (Massopust, 1994) to smoother wavelet functions, as Daubechie's wavelet function "db5" and symmetrical Coiflet wavelet function "coif5". After decomposition the coding gain (c_g) was calculated from variances of decomposed sub-bands:

$$c_g = \sum_{j=1}^{J}(\sigma_j^2 \cdot \alpha_j) / \prod_{j=1}^{J}(\sigma_j^2)^{\alpha_j} \tag{48}$$

where σ_j^2 are variances of sub-bands and α_j are the relative length of sub-band sequences and J the number of sub-bands. The coding gain is a measure of spectral flatness. For (uniform) white noise it has the value 1. Also the Shannon's entropy was calculated and can be viewed as a measure of signal complexity. The numerical experimental results are collected in Table 4.

	c_g, I_2	c_g, white noise	entropy, I_2	entropy, white noise
db2	1.3486	1.0090	4.5384	4.9304
db5	1.3411	1.0076	4.5384	4.9304
coif5	1.3411	1.0116	4.5384	4.9304

Table 4. Coding gain and Shannon's entropy obtained with different wavelet functions

The chose of different wavelets did not influence on the obtained c_g and entropy. We found also, that the coding gain and entropy can be used as an additional parameter to distinguish the corrosion processes.

To study the approximation properties of DWT's using different wavelet basis functions, a synthesis (inverse DWT) to different approximation levels was made. We expected better results with ''db2'' assuming the fractal–like shapes of EN-signals. However, no significant differences were found, a smaller approximation error was obtained even using smoother wavelets, what confirms the approximation theory.

6. Conclusion

The most attractive prospective benefit of EN measurement is the ability to obtain information about the type of corrosion that is occurring, but there is much less agreement

about the optimum analysis method for obtaining such information (Cottis, 2006). Wavelet transform has been developed over a number of years and only recently has been applied to electrochemical noise analysis. The main advantage of wavelet analysis of EN is the detection of transients which are localized in both the time and frequency domain and shows promise to be discriminatory for the intensity as well as the type of corrosion.

7. References

Aballe, A., Bethencount, M., Botana, F. J. & Markos, M. (1999). Using wavelets transform in the analysis of electrochemical noise data, *Electrochimica Acta,* Vol.44, No.26, (September 1999), pp. 4805-4816, ISSN: 0013-4686

Aballe, A., Bethencount, M., Botana, F. J., Markos, M. & Sanchez-Amaya, J. M. (2001). Use of wavelets to study electrochemical noise transients, *Electrochimica Acta,* Vol. 46, No. 15 (April 2001), pp. 2353- 2361, ISSN: 0013-4686

Akay, M., Mulder, E. J. H. (1998). Effects of Maternal Alcohol Intake on Fractal Properties in Human Fetal Breathing Dynamics, *IEEE Transaction on Biomedical Engineering*, Vol. 45, No. 9, (September 1998), pp.1097 – 1103, ISSN: 0018-9294

Attarchi, M., Roshan, M. S., Norouzi, S. & Sadrnezhad, S. K. (2009). Electrochemical potential noise analysis of Cu-BTA system using wavelet transformation, *Journal of Electroanalytical Chemistry,* Vol. 633, No. 1, (2009), pp. 240-245, ISSN: 1572-6657

Banjanin, B., Gergič, B., Planinšič,P. & Čučej, Ž. (2001). Entropy-threshold method for best basis selection, *Image and Vision Computing* Elsevier, Vol. 19, No. 7, (May 2001), pp. 477- 484, ISSN: 0262-8856

Burrus, C. S. (1992). *Introduction to wavelets and wavelet transforms*, *A primer*. Prentice Hall, ISBN: 0-13-489600-9, Upper Saddle River, New Jersey, USA

Cottis, R. A. (2001). Interpretation of Electrochemical Noise Data, *Corrosion*, Vol. 57, No.3, (2001), pp.265-285, ISSN: 0010-9312

Cottis, R.A. (2006). Sources of Electrochemical Noise in Corroding Systems, *Russian Journal of Electrochemistry*, Vol. 42, No. 5, 2007, pp. 497-505, ISSN: 1023-1935

Dai, X., Joseph, B. & Motard, R. L. (1994). Introduction to Wavelet Transform and Time-Frequency Analysis, In: *Wavelet Applications in Chemical Engineering*, Motard, R. L. &Joseph, B., (Eds.), 1-32, Cluwer Academic Publisher, ISBN: 0-7923-9461-5. Norwell, Massachusetts, USA.

Daubechies, I. (1992). *Ten Lectures on Wavelets*, Siam, ISBN: 0-89871-274-2, Philadelphia, Pennsylvania, USA

Farge, M. (1993). *Wavelets, Fractals, and Fourier Transforms*, J. C. Hunt, J. C. Vassilicos (Eds.), Clarendon Press, ISBN: 0-19-853647-X, Oxford, USA

Flandrin, P. (1992). Wavelet analysis and synthesis of fractional Brownian motion, *IEEE Trans. Information theory*, Vol. 38, No.2, Part 2, Mar. 1992, pp.904-909, ISSN: 0018-9448

Flandrin, P. (1993). Fractional Brownian Motion and Wavelets, In: *Wavelets, Fractals, and Fourier Transforms*, Farge, M., Hunt, J. C. R. & Vassilicos, J. C., (Eds.), 109-142, Clarendon Press, ISBN: 0-19-853647-X, Oxford, USA

Gao, Y., Cao, Y., Tung, W.-W. & Hu, J. (2007). *Multiscale analysis of complex time series (Integration of chaos and random fractal Theory, and Beyond)*, John Wiley & Sons, ISBN: 978-0-471-65470-4, New Jersey, USA

Haruna, T., Morikawa, Y., Fujimoto, S. & Shibata, T. (2003). Electrochemical noise analysis for estimation of corrosion rate of carbon steel in bicarbonate solution, *Corrosion Science*, Vol. 45, No. 9, pp. 2093-2104, ISSN: 0010-938X

Kim, J.J. (2007). Wavelet analysis of potentiostatic electrochemical noise, *Materials Letters*, Vol. 61, No. 18, 2007, pp. 4000-4002, ISSN: 0167-577X

Lafront, A.M., Safizadeh, F., Ghali, E.& Houlach, G.(2010). Study of the copper anode Passivation by electrochemical noise analysis using spectral and wavelet

transforms, *Electrochimica Acta* , Vol. 55, No. 22, 2010, pp. 2505-2512, ISSN: 0013-4686

Lee, C. C. & Mansfeld, F. (1998). Analysis of electrochemical noise data for a passive system in the frequency domain, *Corrosion Science*, Vol. 40, No. 6, pp. 959-962, ISSN: 0010-938X

Mallat, S. (1998). *A wavelet tour of signal processing*, Academic Press, 1998. ISBN :0-12-466606-X, San Diego, California, USA

Mansfeld, F., Sun, Z: & Hsu, C.H. (2001). Electrochemical noise analysis (ENA) for active and passive systems in chloride media, *Electrochimica Acta* , Vol. 46, No. 24-25, 2001, pp. 3651-3664, ISSN: 0013-4686

Massopust, P. R. (1994). *Fractal Functions, Fractal Surfaces, and Wavelets*, Academic Press, ISBN: 0-12-478840-8, San Diego, California, USA

Mathworks Inc.(2007), Matlab® 7.5.0 (R2007b), 2007

Muniandy, S.V., Chew, W.X. & Kan, C.S. (2011). Multifractal modeling of electrochemical noise of corrosion of carbon steel, *Corrosion Science*, Vol. 53, No.1, pp. 188-200, ISSN: 0010-938X

Orfanidis, S.J. (1996). *Introduction to Signal Processing*, Prentice Hall, ISBN 0-13-209172-0, Upper Saddle River, New Jersey, USA

Palavajjhalla, S., Motard, R. L & Joseph (1994), B. Computational Aspects of Wavelets and Wavelet Transforms, In: *Wavelet Applications in Chemical Engineering,* Motard, R. L. &Joseph, B., (Eds.), 33-83, Cluwer Academic Publisher, ISBN: 0-7923-9461-5. Norwell, Massachusetts, USA.

Petek, A., Doleček, V. & Vlachy, V. (1997). Stochastic Analysis of Current Fluctuations During General Corrosion of Stainless Steel in Sulfuric Acid, *Corrosion*, Vol. 53, No.12, (1997), pp.928-934, ISSN: 0010-9312

Petek, A: & Doleček, V. (2001). Interpretation of current noise generation by a simple model, *Materials and Corrosion*, Vol. 52, No.6, (2001), pp.426-429, ISSN: 1521-4176 Planinšič, P., Gergič, B., Gleich, D. & Čučej, Ž.(2001). Fuzzy control of subband codded image quality using standard and fuzzy quality measure, *Optical Engineering*, Vol.8, No.40, (August 2001), pp. 1529-1544, ISSN 0091-3286

Planinšič, P. & Petek, A. (2003). Analysis of electrochemical noise signals with classical methods and methods based on fractal-like wavelets, *Proceedings IEEE ICIT 2003*, 871-876, ISBN: 0-7803-7853-9, Maribor, Slovenia, December 10-12, 2003

Planinšič, P. & Petek, A. (2004). Analysis of electrochemical noise signals using fractal-like function wavelets, In: *Interdisciplinary applications of fractal and chaos theory,* R. Dobrescu, C. Vasilescu, (Ed.), 322-334, Editura Academica Romane, ISBN 937-27-1070-5, Bucaresti, Romania

Planinšič, P. & Petek, A. (2007). Electrochemical noise signals discrimination using wavelet-based fractal analysis, *Proceeding of 3rd international symposium on Interdisciplinary*

approaches in fractal analysis IAFA 2007, pp. 322-334, ISBN 842-6508-23-3, Printech, Bucaresti, Romania, May 23-25, 2007

Planinšič, P. & Petek, A. (2008). Characterization of corrosion processes by current noise - based fractal and correlation analysis, *Electrochimica Acta,* Vol. 53, No. 16, June 2008), pp. 5206-5214, ISSN: 0013-4686

Sekine, M., Tamura, T., Akay, M., Fujimuto, T., Togawa, T. & Fukuji, Y. (2002). Discrimination of Walking Paterns Using Wavelet-Based Fractal Analysis, *IEEE Transaction on Neural Sysems and rehabilitation Engineering,* Vol.6, No.3, (September 2002), pp. 188 -196, ISSN: 1534-4320

Shi, Y.Y., Zhang, Z., Cao, F.H. & Zhang J.Q. (2008). Dimensional analysis applied to pitting corrosion measurements, *Electrochimica Acta* , Vol. 53, No.6, 2008, pp. 2688-2698, ISSN: 0013-4686

Schroeder, M. (1991). *Fractals, Chaos, Power Laws (Minutes from an Infinite Paradise)*, W. H. Freeman and Company, ISBN: 0716721368, New York, USA

Smulko J., Darowicki, K. & Zielinski, A. (2002). Pitting Corrosion in Steel and Electrochemical Noise Intensity, *Electrochemistry Communication*, Vol. 4, No. 5 (May 2002), pp 388-391(4). ISSN: 1388-2481

Wharton, A., Woo, R. J. K. & Mellor, B. G. (2003). Wavelet analysis of electrochemical noise measurements during corrosion of austenitic and superduplex stainless steels in chloride media, *Corrosion Science*, Vol. 45, No. 1, (January 2003), pp 97-122. ISSN: 0010-938X

Wornell, G. W. (1996). *Signal Processing with Fractals, A Wavelet–Based Approach*, Prentice Hall PTR, ISBN 013120999X, Upper Saddle River, New Jersey, USA

Zhang, T., Shao, Y., Meng, G. & Wang, F. (2007). Electrochemical noise analysis of the corrosion of AZ91D magnesium alloy in alkaline chloride solution, *Electrochimica Acta* , Vol. 53, No.17, 2007, pp. 561-568, ISSN: 0013-4686

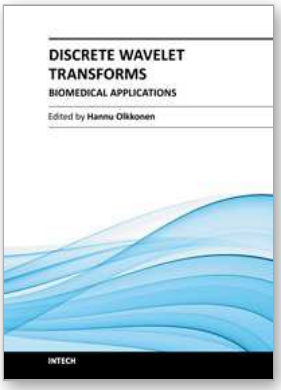

Discrete Wavelet Transforms - Biomedical Applications

Edited by Prof. Hannu Olkkonen

ISBN 978-953-307-654-6
Hard cover, 366 pages
Publisher InTech
Published online 12, September, 2011
Published in print edition September, 2011

The discrete wavelet transform (DWT) algorithms have a firm position in processing of signals in several areas of research and industry. As DWT provides both octave-scale frequency and spatial timing of the analyzed signal, it is constantly used to solve and treat more and more advanced problems. The present book: Discrete Wavelet Transforms - Biomedical Applications reviews the recent progress in discrete wavelet transform algorithms and applications. The book reviews the recent progress in DWT algorithms for biomedical applications. The book covers a wide range of architectures (e.g. lifting, shift invariance, multi-scale analysis) for constructing DWTs. The book chapters are organized into four major parts. Part I describes the progress in implementations of the DWT algorithms in biomedical signal analysis. Applications include compression and filtering of biomedical signals, DWT based selection of salient EEG frequency band, shift invariant DWTs for multiscale analysis and DWT assisted heart sound analysis. Part II addresses speech analysis, modeling and understanding of speech and speaker recognition. Part III focuses biosensor applications such as calibration of enzymatic sensors, multiscale analysis of wireless capsule endoscopy recordings, DWT assisted electronic nose analysis and optical fibre sensor analyses. Finally, Part IV describes DWT algorithms for tools in identification and diagnostics: identification based on hand geometry, identification of species groupings, object detection and tracking, DWT signatures and diagnostics for assessment of ICU agitation-sedation controllers and DWT based diagnostics of power transformers.The chapters of the present book consist of both tutorial and highly advanced material. Therefore, the book is intended to be a reference text for graduate students and researchers to obtain state-of-the-art knowledge on specific applications.

How to reference

In order to correctly reference this scholarly work, feel free to copy and paste the following:

Peter Planinšič and Aljana Petek (2011). Wavelets in Electrochemical Noise Analysis, Discrete Wavelet Transforms - Biomedical Applications, Prof. Hannu Olkkonen (Ed.), ISBN: 978-953-307-654-6, InTech, Available from: http://www.intechopen.com/books/discrete-wavelet-transforms-biomedical-applications/wavelets-in-electrochemical-noise-analysis

INTECH
open science | open minds

InTech Europe
University Campus STeP Ri
Slavka Krautzeka 83/A

InTech China
Unit 405, Office Block, Hotel Equatorial Shanghai
No.65, Yan An Road (West), Shanghai, 200040, China

51000 Rijeka, Croatia
Phone: +385 (51) 770 447
Fax: +385 (51) 686 166
www.intechopen.com

中国上海市延安西路65号上海国际贵都大饭店办公楼405单元
Phone: +86-21-62489820
Fax: +86-21-62489821